Local computational resources at BGSU

Alexey T. Zayak
Department of Physics and astronomy
Bowling Green State University

July 3, 2018

In-house resources

Our group at BGSU has a small computational laboratory equipped with several personal workstations running Linux. For testing purposes and small calculations we have our own local cluster, called “Bethe” which is hosted and managed by the Information and Technology Center at BGSU. The cluster has 8 computing nodes, each with two 8-code Xeon E5 processors, with 8 GB of RAM per core.

The cluster is actively used for small computations or larger calculations that require very long run time, like MD simulation. Although, the cluster is 5 yeas old (it was purchased in 2012), it is still fully functional and helps our groups to maintain research. However, this is clearly not a production machine. First, is it too small for most of our projects, second a lot of time on ”Bethe” is taken by undergraduate students who are being trained in our group.

- PSSC Labs PowerWulf MMx Cluster “Bethe”
- Configuration:
- 128 compute cores (Intel Xeon E5-2650)
- 576 GB System RAM (512 GB RAM for compute nodes)
- 16TB Hard Drive storage
- QDR InfiniBand Network

In addition to ”Bethe” our group uses two powerful personal workstations (purchased in 2012):

- PSSC Labs workstation:
- 2x6-cores, 2.0-GHz Xeon E5-2600 CPU,
- 64 GB RAM
- 2TB 6Gbps HDD
- nVidia GeForce with 1GB

Overall, our in-house computational resources are more than limited. They are suitable for training students and performing test calculations, but absolutely insufficient for the research computations that our group does (DFT based electronic structure).

Other resources

The group used to actively utilize the resources available through the Ohio Supercomputer Center (OSC). Our annual usage was on the order of 1,200,000 CPU hours, which was a very significant part of our computing power, on par with our XSEDE allocation. All our computations were done at OSC and XSEDE (TACC). However, OSC is not available for our research any more. Starting from July 1, 2018, OSC switches to a charge-based system, when users have to pay actual money for the utilized resources. Since BGSU does not have funds for this kind of expenses, OSC is not available for our research any more. Starting from July 1, 2018, XSEDE is the only computational resource that we have.

Progress report

Vibrational Spectroscopy of Heterogeneous Chemical Interfaces

Alexey T. Zayak
Bowling Green State University

1 Overview of the project

Our 2017 allocation was used to conduct deep fundamental studies of the interfacial chemical phenomena that occur between inorganic surfaces and organic adsorbates. At the same time, we tested our computational approach on real-life applications, like our glucose detection project, which will be described below. The key aspect of our research is that the use of the Surfaced Enhanced Raman Scattering (SERS) can reveal spectroscopic information from such interfaces that are unmatched by any other existing technique. A major challenge for studying heterogeneous systems is the characterization of the dipole layer that is formed in any heterogeneous interface, simply due to the fact that one system donates charge to another. In order to understand the properties of such systems one needs a way of estimating the amount of charge transfer across the interface. In order to solve this problem, we explore the yet unknown capabilities of Raman spectroscopy. In the following section, we will discuss our results that have been obtained so far using the resources from XSEDE.

2 Previous and current results from our work at XSEDE

- A. K. Kuhlman, A. T. Zayak, "Revealing interaction of organic adsorbates with semiconductor surfaces using chemically enhanced raman," *J. Phys. Chem. Lett.*, **5** (6), 2014, pp. 964-968
- G. B. Bhandari, K. Subedi, Y. He, Zh. Jiang, M. Leopold, N. Reilly, H. P. Lu, A. T. Zayak, and L. Sun, "Thickness-Controlled Synthesis of Colloidal PbS Nanosheets and Their Thickness-Dependent Energy Gaps", *Chem. Mater* **26** (19), 2014, pp 5433-5436
- F.W. Hilty, A.K. Kuhlman, F. Pauly, and A.T. Zayak, "Raman Scattering from a Molecule-Semiconductor Interface Tuned by Electric Field: Density Functional Theory Approach." *J. Phys. Chem. C* **119** (40) 2015, pp 23113-23118
- Keshab Bashyal, Christopher K. Pyles, Sajjad Afroosheh, Aneer Lamichhane, and Alexey T. Zayak, "Empirical optimization of DFT + U and HSE for the band structure of ZnO", *J. Phys.: Condens. Matter* **30** (2018) 065501
- (in preparation) A. T. Zayak. C. Pyles, B. Chunesh, P. Darancet, "Quantifying Interfacial Charge Transfer with Surface - Enhanced Raman Scattering." *to be submitted in 2018*
- (under review) D. Yang, S. Afroosheh, J. O. Lee, H. Cho, S. Kumar, Y.-Z. Yoon, A. T. Zayak, H. Choo, "Demonstration of Intraocular Label-Free Glucose Sensing using Raman-Mode Constraining" under review in ACS Analytical Chemistry

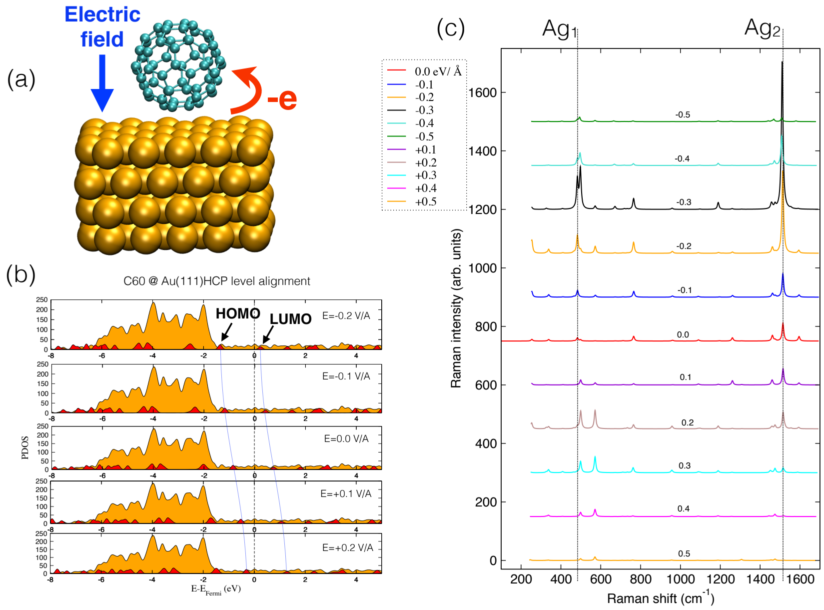

Figure 1: (a) The slab geometry supercell simulated in this project with the C60 molecule adsorbed on Au(111) surface. Upon adsorbtion to the surface the molecule exchanges some charge with the surface, the amount of which can be tuned by applying external electric field. (b) Response of the electronic structure to the applied electric field. (Only a few values of electric biases are shown to save space.) (c) Raman spectra computed for the system shown in panel (a) at various external electric biases.

3 Ongoing projects

3.1 PROJECT 1: Quantifying the charge transfer: C60 on gold(111)

In this project, we proposed that Raman intensities as well as corresponding shifts of vibrational frequency can be used to for quantifying the charge transfer across heterogeneous interfaces.

Figure 1 shows our results for the Raman spectra of a C60 molecule adsorbed on Au(111). It is probably the most expensive Raman calculation that has been done so far. Overall, it took us more than two years to obtain the data shown in Fig.1(c). The challenge of this project arises from working with a real extended gold surface (represented by a slab geometry in SIESTA). The structure shown in Fig.1(a) is not a cartoon, but the actual unit cell used in our simulations, plus 40 Å of vacuum added in the vertical direction. In addition to the big size, our calculations are required to handle carefully both large external electric biases and additional small perturbations of the electric field for computing electronic polarizability.

Currently, we are working on the rationalization of the non-trivial trend that is shown in Fig.1(c). We note that in the case of negative biases, the charge transfer occurs from the metal surface to the LUMO state of the molecule, while under positive biases the charge flows from the HOMO state of the molecule to the metal. The computed spectra contain information not only about the dipole layer charge transfer that occurs at every bias value, but also about the dynamical coupling of each vibrational mode to the charge transfer across the interface. Understanding of this behavior based on the electronic structure of the interface is the ultimate goal of this work. We expect this work to be submitted by the end of Summer 2018. NSF proposal focused on this work is being under review. If not funded in this cycle, it will be resubmitted in the fall 2018 with the exciting preliminary data shown in Fig.1(c).

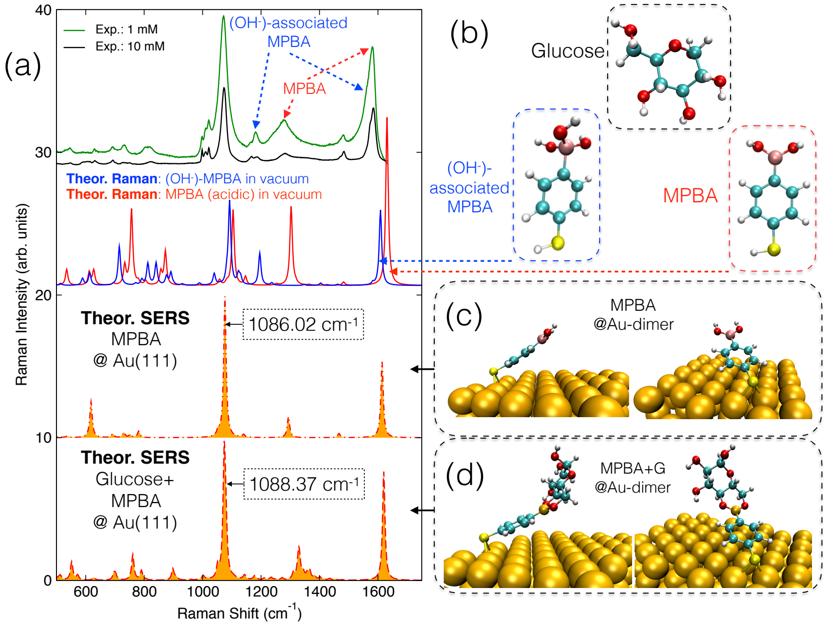

Figure 2: (a) (From top to bottom) Experimental spectra of MPBA obtained by the Caltech group for two concentrations of MPBA. Calculated Raman spectra of isolated (gas phase) molecules MPBA and (OH-)MPBA. SERS spectra of MPBA on Au(111). SERS spectra of MPBA+Glucose on Au(111). (b) Atomic structures of glucose, MPBA and (OH-)MPBA. (c) Atomic structure of MPBA adsorbed on Au(111). (d) Atomic structure of MPBA+Glucose on Au(111).

3.2 PROJECT 2: Glucose detection using Raman spectroscopy

While we mostly aim for fundamental understanding of the interfacial Raman spectroscopy, sometimes our expertise can be beneficial for real-life applications. The group of Dr. Hyuck Choo (Caltech) discovered a novel signature that allows for accurate non-invasive detection of glucose in living biological systems using Raman scattering. While the effect has been established experimentally by the Caltech group, underlying physical (chemical) mechanisms were unknown.

We carried out an extensive computational study using Stampede in order to reveal the mechanism with a specific spectroscopic signature that allows for unambiguous glucose detection. The computational work required not only explicit modeling of an extended gold surface of the SERS sample, but also an explicit solvent representing a realistic biological environment (675 atoms in total). The latter is essential to correctly simulate the signaling linker molecule 4-mercaptophenyl boronic acid (MBPA), which exists in two distinct forms: neutral and charged (OH-)- associated, with the relative contributions strongly dependent on the pH value. Raman simulations of such complex systems have never been done before. This project underlines the critical methodological aspect of employing a proper solvent model for reproducing correct SERS spectra of charged species, while the neutral ones can be successfully computed in the vacuum.

Figure 2 shows some results and illustrates the approach. In Fig.2(a) the top graph shows the experimental data for the linker molecule, MPBA, adsorbed on gold surface. Our calculations shown right below the experimental data reveal that the experiment measures roughly 50/50 composition of the two types of the linker molecule. This is an important observation, because the ratio between the two types of MPBA is pH-dependent. A reliable approach for glucose detection must be invariant to the type of the linker molecule. Our calculations of real SERS data for MPBA and MPBA+glucose on gold surface, shown in Fig.2(a) show that glucose binding causes a detectable blue-shift of one particular vibrational peak around 1080 cm^{-1}. This mechanism has been verified by our collaborators at Caltech with a publication being under review in Analytical Chemistry.

Scaling information for Stampede-2

Alexey T. Zayak
Department of Physics and astronomy
Bowling Green State University

July 10, 2018

The proposed work will be mainly based on the usage of two well-known software packages SIESTA and VASP. We also do some benchmarking using Quantum Espresso, but those calculations are usually small and can be done on our local computers. Both SIESTA and VASP packages exist on Stampede2 as loadable modules, but we also have successfully compiled our own versions with custom modifications (thanks to the help from TACC!).

SIESTA

SIESTA is our main tool in this project. Our choice of this code is based on the efficiency of dealing with slab geometries. Our calculations of electronic polarizabilities require a significant amount of vacuum space separating periodic images of slabs. Using plane-waves based software, like VASP or Quantum Espresso, is very computationally expensive. On the other hand, localized orbitals used by SIESTA are remarkably efficient for such systems.

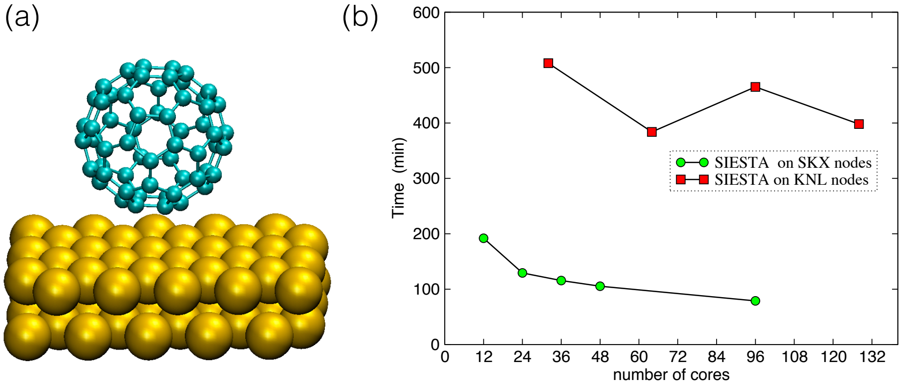

Figure 1: C60 on Au(111)

Scaling of SIESTA on Stampede2 is not so impressive. Figure 1 shows the scaling information obtained for our major system of study, C60 molecule adsorbed on Au(111) surface. We should note that this is a rather big system for DFT-based computations, but SIETSA makes this system manageable, even with hundreds of calculations required to vibrational dynamics and Raman scattering.

The SKX nodes are quite familiar to us. We have worked with similar nodes on Stampede1 and know that the scaling shown in Fig. 1 is normal. Overall, the SKX processors on Stampede2 are remarkably fast for our SIESTA jobs. Considering the presented scaling behavior, we usually take 24 cores (one processor) per job, and use the second processor to run another similar job at the same time, using the concurrent execution of

MPI jobs, which is available on Stampede2. This way, we almost double the efficiency of our computations. For smaller systems, like an isolated molecule, we ran four concurrent jobs on the same node. Please, see the ”Divide and Conquer” section in the end of this document.

The KNL nodes do not cooperate with our SIESTA-based calculations. Until now, we just run test calculations and will request help from TACC to improve the compilation on KNL nodes. One can see in Fig. 1 that one entire KNL node is about 3 times slower than an entire SKX node. But also, we see a significant kink (drop of efficiency) when we go beyond a single node.

VASP

VASP is not our major code, we use it less than SIESTA, but VASP calculations are more expensive. Good scaling is more critical here, and so far we see very respectable scaling on both SKX and KNL nodes.

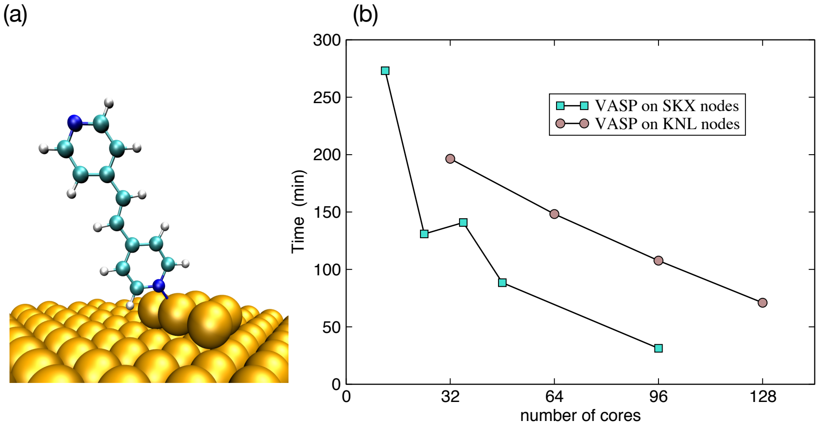

Figure 2: VASP BPE on Au(111).

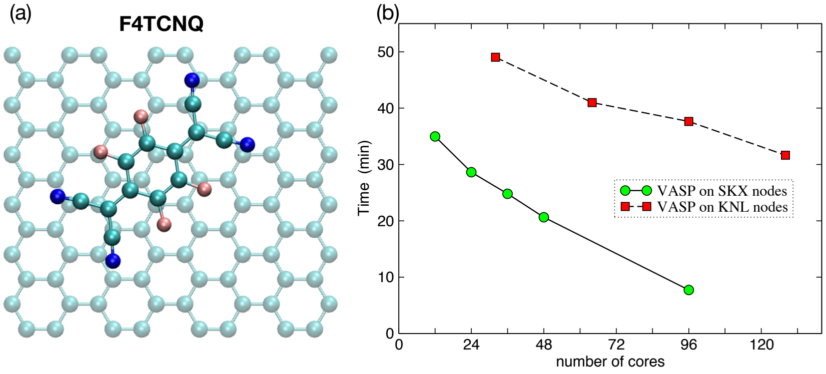

Figure 3: VASP F4-TCNQ

Figures 2 and 3 show scaling trends for two typical systems: trans-1,2-bis(4-pyridyl)ethylene (BPE) adsorbed on Au(111) with 4 layers of Au atoms; and F4-TCNQ molecule physisorbed on graphene. For both systems, VASP runs faster on SKX nodes, but still KNL nodes show good scaling trends. We should note that in order to simplify this analysis, we did not change the NPAR parameter in VASP (keeping it NPAR = 4). It is well known that VASP allows for some tuning of the scaling behavior, which may lead to even better performance.

“Divide and Conquer” methodology

The key aspect of our Raman calculations is that we do not need to run very large calculations. Instead, we use the “Divide and Conquer” approach and run big numbers of independent calculations, which later assemble to computed vibrational parameters and Raman spectra. In this respect our calculations are trivially parallel. While typically for a single DFT calculation we would choose 24-48 cores, depending on the size of a particular system, simultaneous execution of many configurations significantly reduces the overall time-span of our projects. Our previous experience shows that the overall use of large computational resources is going to be very efficient. We do not need to run big jobs, but rather hundreds or relatively small jobs. We would like to point out that some of our single-point calculations are very short, taking less than 2-4 hours, which feels many holes in the queues on Stampede2. Our waiting time is typically quite short due to the small size (one node per job) and short wall time.

Concurrent execution

As it was mentioned above, most of our jobs are small-size, but they are very many, hundreds for just a single Raman spectrum. In order to improve the “Divide and Conquer” approach, we actively utilize the `tast_affinity` script, which allows for concurrent executions of multiple jobs on a single node. Below, we provide an example of our script tht runs two concurrent calculations on a single SKX node. The same approach works very well on the KNL nodes.

```
 #!/bin/bash
#SBATCH -J p0.5
#SBATCH -o ATZ_am.o%j
#SBATCH -N 1
#SBATCH -n 48
#SBATCH -p skx-normal
#SBATCH -t 02:00:00
#SBATCH -A TG-DMR130080

cd ./MINUS
cd ./PZ
ibrun -n 24 -o 0 task_affinity $HOME/bin/siesta4.1 < input.fdf > scf.out &
cd ../
cd ../

cd ./PLUS
cd ./PZ
ibrun -n 24 -o 24 task_affinity $HOME/bin/siesta4.1 < input.fdf > scf.out &
wait
cd ../
cd ../
```

Conclusions

Overall, our software is well-behaved and efficient on Stampede2, but the key advantage of our calculations is the “Divide and Conquer” approach, which utilizes the large computational facilities most efficiently. For example, our calculation of Raman spectrum for the system shown in Fig. 1(a) requires 2832 single-point electronic structure calculations. On a 12-core parallel workstation that we have at BGSU, one such calculation takes about 6 hours. For all 2832 calculations we would have to wait for 708 days, which makes research impossible. On Stampede2 we get our results within a week or two, depending on the state of the queue.

Project Summary

Vibrational Spectroscopy of Heterogeneous Chemical Interfaces

This project is a continuation of our current computational research at BGSU in the field of vibrational spectroscopy of heterogeneous interfaces. In the 2018 research window, we aim to utilize the Chemically-Enhanced (CE) Raman scattering for measuring the interfacial coupling between surfaces and non-covalently bound adsorbates. The motivation for this study arises from the recent advances in the understanding of CE mechanism in Raman, which clearly reveals the role of charge transfer. With this new knowledge Raman spectroscopy has a potential for becoming an analytical tool in conjunction with the Surface Enhanced Raman Scattering (SERS).

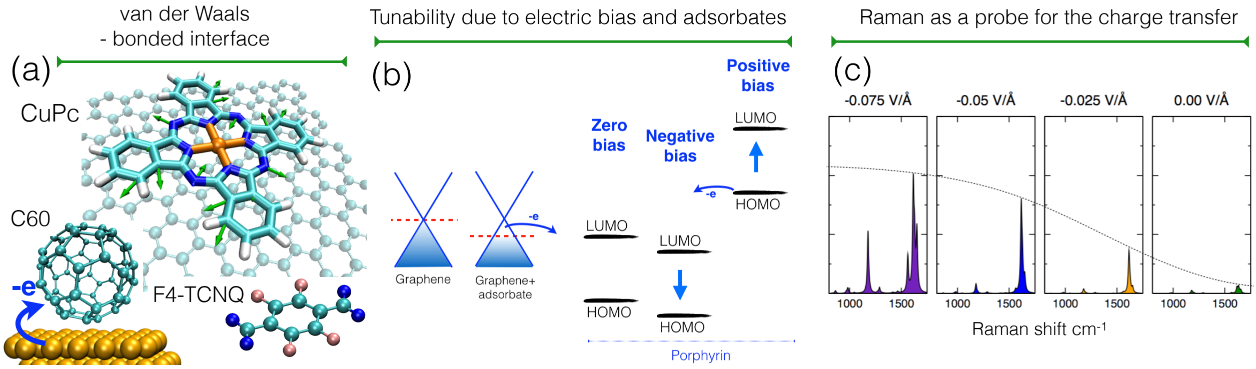

Figure 1: (a) Porphyrin (CuPC) on graphene, C60 on (111)Au; and F4-TCNQ molecule. (b) Schematic representation of the graphene electronic structure and the relative positions of the HOMO and LUMO of the adsorbate tuned by external biases. (c) A representative bias-dependent Raman spectrum calculated with our SIESTA-based methodology.

The existing studies on the CE effect have been focused mainly on the covalently bound adsorbates. A strong covalent bond yields a stronger CE effect in Raman. Not much is known about the CE-effect in non-covalently interacting adsorbates in this regard. Non-covalently bonded assemblies represent a significant portion of actively investigated interfaces, for example, porphyrins adsorbed on graphene or metals. Experimental evidence suggests that the interfacial dipole layer along with the electron-phonon coupling are significant in such systems, which should be revealed by the CE-based analysis of Raman/SERS/GERS measurements.

The particular systems of interest are:

1. *C60 on gold(111) and silver(001) surfaces.* Experimental data suggest different amounts of charge transfer between the molecule and these two metals. Simple interfacial morphology of the interface reduces the number of unknowns and allows for a straightforward correlation between the interfacial charge transfer and the Raman spectra.

2. *TCNQ/F_4TCNQ on graphene.* This organic adsorbate is known to accept about 0.3 electrons from graphene per molecule, making graphene p-doped and creating an interfacial dipole layer. The electron-phonon coupling at the interface is expected to modulate the charge balance at the interface, modifying the Raman signature of this system.

3. *Porphyrin (CuPC) on graphene.* Large Raman scattering cross section makes this molecule a benchmark system for graphene-based Raman (GERS), and a photo-active model for numerous applications.

As the outcomes, we will establish case by case guidelines for a new type of spectroscopic analysis based on Raman chemical enhancement, with the focus on the interfacial charge transfer and dynamics. This analytical approach may become a new Raman imaging technique for studying surfaces and heterogeneous interfaces.

1 BACKGROUND

1.1 The Zayak lab

Zayak (PI) has a substantial experience in the field of computational Raman scattering, especially focused on the aspects of the Chemical Enhancement (CE). Zayak has published four research papers about the CE - based analysis of Raman scattering on metallic and semiconductor surfaces. Currently, the research group of Zayak is developing better and more efficient computational approaches for studying surface Raman scattering, both non-resonant and resonant, in the presence of explicit solvents. Graduate students in the lab are trained in Physics and Photochemistry pathways and create an interdisciplinary blend of experiences in modeling materials properties.

1.2 Literature review

1.2.1 Surface Enhanced Raman Scattering and the Chemical Enhancement

Raman spectroscopy would be a very desirable technique due to its high sensitivity to the atomic structure of materials and to their local environment (Ferraro et al., 2003). However, due to its fundamentally small scattering cross section and the diffraction of light limitations (Schuck et al., 2013), it was not actively used at the nanoscale until the discovery of the plasmon-assisted surface - and tip - enhanced Raman spectroscopies (SERS/TERS) (Stiles et al., 2008; Kim & Shin, 2011). Nowadays, the plasmon-assisted Raman scattering is widely used in various areas of the nano-scale imaging (Stewart et al., 2012). When it comes to Raman spectroscopy of heterogeneous systems, there are more aspects of the electron-vibron interactions that we do not fully understand, and therefore do not use that information from Raman spectra. Specifically, it would be very beneficial to acquire a deeper understanding of the effect called "Chemical Enhancement" (CE), which is, in essence, the reflection of the adsorbate-surface electron-phonon coupling (Moskovits, 2013, 1985).

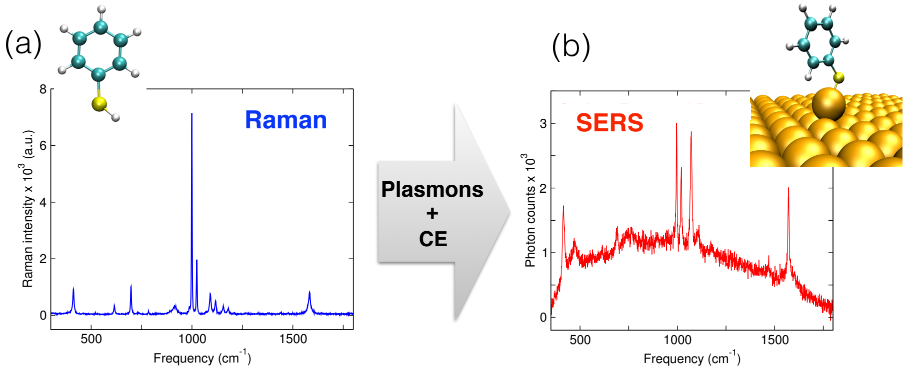

Figure 2: (a) Raman spectrum of benzene thiol molecule in solution. (b) SERS spectrum of benzene thiol taken on gold surface.

Soon after the discovery of SERS (Fleischman et al., 1974; Jeanmaire & Duyne, 1977), it was understood that the chemical modification of Raman spectra is a general phenomenon and must occur on many types of surfaces (Campion & Kambhampati, 1998). Figure 2 shows examples of a conventional Raman spectrum of the benzenethiol molecule and the corresponding SERS spectrum of the same molecule. One can see that the two spectra look quite different. This difference makes sense because a molecule bound to the surface becomes to some extent a different chemical species (Moskovits, 2013). It has been understood that the dynamic charge transfer induced by the local electron-vibration coupling plays an important role in CE (Adrian, 1982; Lombardi & Birke, 2007).

1.2.2 Computational advances in Raman and CE

On the computational side, the methodologies for calculating non-resonant and resonant Raman spectra have been significantly improved as well (Jensen et al., 2008, 2007, 2005; Saikin et al., 2010). Jensen and Schatz introduced a two-state approximation (Jensen et al., 2005), which allows for a simpler interpretation of the Raman spectra computed with DFT (Zayak et al., 2011). The two-state model is somewhat oversimplified, but it is amazingly useful for interpreting experimental and especially DFT data (Zayak et al., 2011; Valley et al., 2013). It shows that the overall CE contribution is given by the value of lowest excitation energy ω. Then, the overall enhancement is multiplied by the second factor $^{\partial\omega}/_{\partial Q_n}$, which we can call as a deformation potential. It is different for every vibration mode and leads to the different Raman spectrum profile when comparing conventional Raman and SERS data (Zayak et al., 2011). Figure 3 shows the simplified two-state view on the CE mechanism for the case of the benzenethiol spectra shown previously in Fig. 2.

The overall enhancement factor is a big challenge, being a function of the electronic level alignment shown in Fig. 3(a). Not only the accurate level alignment is a challenge for the computational theory (Moore et al., 2012), but also it depends on the unknown (and therefore empirical) value of the damping parameter Γ (Jensen et al., 2005), also mentioned previously by Lombardi (Lombardi & Birke, 2007). Having such an empirical parameter in the electronic structure calculations of Raman leaves the quantitative assessment of CE as an open question. Even more problematic our preliminary results for C60 on Au(111) surface show that the damping parameter is also a function of the vibrational amplitude, $\Gamma(Q^n)$.

While the overall chemical enhancement remains a big challenge, the two-state model predicts quite well the relative mode-dependent enhancements, given by the derivative term $^{\partial\omega}/_{\partial Q_n}$. Figure 3(c) shows a convincing agreement between the DFT-based predictions and the actual measurements from the literature.

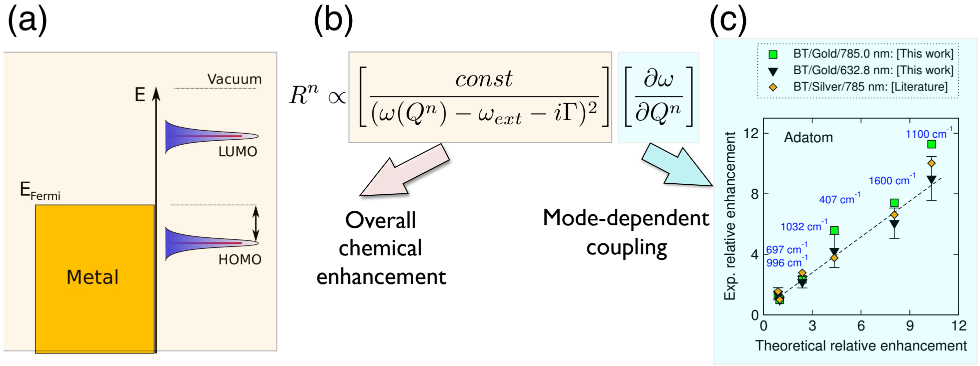

Figure 3: (a) Schematic representation of the interfacial energy levels alignment between a metal surface and an organic adsorbate. (b) The two-state model. (c) The relative experimental and theoretical mode-dependent CE effect for benzene thiol on gold from Ref.(Zayak et al., 2011).

To complete this picture, one should mention the work done by Patrick El-Khoury and co-authors, who take a different approach for calculating Raman and SERS spectra. They use *ab-initio* Molecular Dynamics (AIMD) and Fourier transforms to compute the vibrational densities of states and the Raman spectra, using the velocity and the polarizability autocorrelation functions, respectively (Fischer et al., 2017). This approach yields an impressive agreement with experimental data and allows for incorporating explicit solvents via the QM:MM method (El-Khoury & Hess, 2013). The AIMD simulations of Raman yield a more realistic representation of the experimental situation, which is dynamic. On the other hand, the static approach employed by Zayak and other researchers allows for a ”cleaner” analysis, being based on the fully relaxed structures. Nevertheless, real systems are not necessary ”clean,” and the AIMD approach is perfect for assessing the ”messy” non-equilibrium effects.

2 METHODS

The key aspect of our computational approach is that we study extended surfaces as apposed to approximating surfaces by finite clusters. Experts in the field would know that computing Raman on extended periodic surfaces is rather expensive. It does not mean that our approach is better than the relatively cheaper use of finite clusters. In fact, we also do many calculations with clusters, when aiming to do a quick check of a concept. But clusters usually do not give an accurate representation of the real surface electronic structure, and their structures are frequently ambiguous. Contrary to that, extended surfaces give well defined atomic morphologies and electronic structures of the real material, which greatly simplifies analysis of the data. Thus, at a significantly higher computational cost, we obtain a more definite physical picture.

Calculations in this project will be performed using the density functional theory (DFT) (Kohn, 1999). Our choice of software is the code, SIESTA (http://departments.icmab.es/leem/siesta/), a freely available software package for electronic structure calculations in physics and chemistry (Soler et al., 2002). SIESTA uses numerical atom-centered orbitals as the basis describing wave functions of the system. Properties of atomic species are presented by pseudopotentials of various flavors. Similar to many solid-state-physics oriented codes, SIESTA uses three-dimensional periodic space, which means that semiconductor slab and a molecule adsorbed on this slab are presented by a supercell that has to be large enough in order to avoid interactions between periodic images, which is already a well - tested approach, leading to accurate results. For this particular project, we need to be able to accurately calculate forces for optimizing the structural configuration of the molecule-semiconductor interface and for obtaining vibrational properties. Also, the code has to be capable of applying external electric field. We have shown that SIESTA is well suited for this type of tasks (Kuhlman & Zayak, 2014).

Vibrations will be computed using our own set of scripts, which were tested in a number of previous projects (Zayak et al., 2011, 2012). Our scripts are independent of the DFT software. We can easily use VASP, SIESTA or any other code that provides accurate forces. We construct the dynamical matrix of the system by finite differences, i.e. displacing each atom from the equilibrium position along Cartesian directions by 0.03 Å. We use Hellmann-Feynman forces induced on all atoms of the system to construct a symmetrized form of the dynamical matrix (Postnikov et al., 2005). This approach was described in detail in Ref. Zayak et al. (2011), with all equations given in the Supplementary Materials of that PRL.

The diagonalization of the dynamical matrix leads to frequencies and corresponding normalized mass-weighted eigenmodes for atomic displacements. When calculating Raman, we use the whole-mode approach, where instead of displacing each atom one by one, we freeze-in the entire vibrational mode and then calculate the polarizability. Freezing the entire vibrational mode is very useful from the point. We can follow the process of interfacial vibrational coupling by means of observing the behavior of the charge density and its response to the electric field.

Raman cross sections are computed from the Raman tensor, which is computed for each vibrational mode separately as a derivative of the polarizability tensor with respect to the vibrational displacement vector of that particular mode. In order to compute the polarizability we will use the electric dipole provided by SIESTA, and compute the first derivative of the dipole with respect to a finite electric field using the finite difference method (Umari & Pasquarello, 2005). The standard expression is used for calculating the differential Raman cross section (Cardona & Güntherodt, 1982; Neugebauer et al., 2002). A detailed description of this procedure was given in the Supporting Materials in Ref. Zayak et al. (2011).

3 PROPOSED RESEARCH ACTIVITIES

3.1 PROJECT 1: Interfaces with non-bonding coupling

3.1.1 Methodological details

Our Raman machinery, based on the SIESTA package, is well - suited for studying systems like C60@Au(111). This system is very large and expensive in terms of the computer time. The C60 molecule (60 carbon atoms) needs to be placed on a relatively large metal surface to avoid interactions between neighbor molecules, resulting in 60 Au (or Ag) atoms per layer. Our preliminary results are based on representing the metal slab by two atomic layers only, which might not be sufficient. Calculating Raman spectra for 60 carbon and 120 gold atoms is expensive. We should note that in order to properly describe the metallic properties of the metal, we have to use a suitable mesh of *k*-points for the Brillouin zone integration. Calculations with the Γ-point show unsatisfactory results for the metal surfaces.

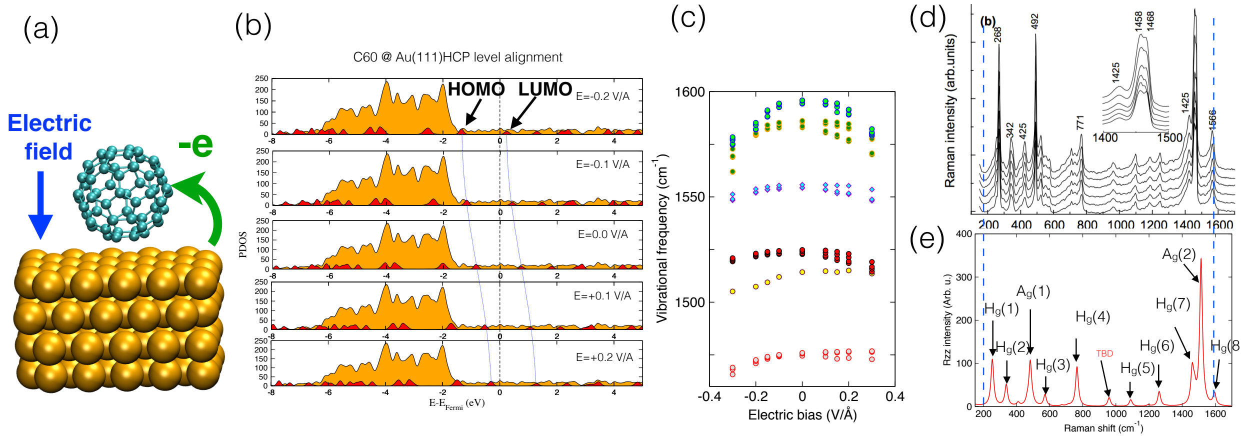

Figure 4: (a) The slab geometry supercell simulated with the C60 molecule adsorbed on the Au(111) surface. Upon adsorption to the surface, the molecule exchanges some charge with the surface, the amount of which can be further tuned by applying an external electric field. (b) Response of the electronic structure to the applied electric field. (c) Computed vibrational frequency shifts plotted as a function of the applied bias. (d,e) Comparison of experimental and calculated SERS spectra for C60 on the Au(111) surface. The experimental data is adopted from Ref. (Baibarac et al., 2005).

Preliminary results of our Raman calculations of C60 on a periodic (flat) gold surface are shown in Fig.4. We note that the flat surface is expensive, but it presents significant advantages over small clusters due to the flat unambiguous topology of the surface. C60-Au-cluster calculations would be cheaper, but the analysis would drastically depend on a particular configuration of the cluster and the particular contact realization between the molecule and the cluster. We had to establish an efficient method for computing SERS spectra of supported molecules on flat surfaces, sketched in Fig. 4(a). Our methodology allows for calculating Raman spectra of such hetero-interfaces in the presence of external electric biases, which enables studying of the effect of the interfacial electronic level alignment in the Raman scattering process. By applying an external bias, we can tune either the HOMO or the LUMO states of the molecule to be in resonance with the metal, shown in Fig. 4(b). Similarly to the predictions from Ref.(Li et al., 2014), we obtained downshifting of the vibrational frequencies of C60 on Au(111) under the applied biases. That indicates that we have and control the charge transfer between the molecule and the surface.

3.1.2 Proposed work

1. ***Extract and understand the charge transfer contribution to the Raman spectra of C60@Au(111) in the presence of external biases.***

As one can see from our progress report, we have already computed vibrations and corresponding Raman spectra of C60@Au(111) for a range of external electric biases: -0.5, -0.4, -0.3, -0.2, -0.1, 0.0, 0.1, 0.2, 0.3, 0.4, 0.5 V/Å. The computed Raman spectra present non-trivial behavior of both vibrational frequencies and spectral intensities as a function of the applied bias. This behavior is entirely mode-dependent, i.e. each vibrational mode has its unique strength and type of coupling. At this point, we are ready to reveal the underlying charge dynamics associated with each vibrational mode.

Expected outcomes

- The proposed computations will provide data for a detailed analysis of the connection between the electronic level alignment (shown in Fig. 4(b)), the Raman intensities, and the corresponding charge transfer. The level alignment picture will enable "reading" the amount of the charge transfer from the densities of states, similar to how it was done in Ref. (Li et al., 2014).

- By applying external electric biases, we drive the system from the coupling dominated by the HOMO to the coupling dominated by the LUMO state. Such modulation can be important because the HOMO and LUMO of C60 have different symmetries and degeneracies, which means that they will couple differently to vibrational modes of different symmetries. On the practical side, that means that Raman spectra may be able to show whether the interfacial coupling is dominated by one of another molecular state.

2. ***Compute Raman spectra of C60@Ag(100)***

It the previous section, we wrote that the tuning of the interfacial coupling with external electric biases would reveal the trends connecting the interfacial coupling with corresponding Raman signatures. However, there is another way of elucidating the role of the substrate-molecule coupling by comparing Au with Ag. In the previous literature, it was shown that unlike the case of Au(111), when C60 is placed on Ag(100) surface, there is charge transfer from the surface to the molecule in the amount of about 0.2 electrons. Thus, a direct comparison between the two noble metals will provide us with another angle of view on the connection between the electronic structure of the interface and the corresponding Raman response.

Expected outcomes - This calculation will present a direct evidence for the impact of the interfacial dipole layer on the Raman spectra of the system. The advantage of comparing the Au(111) and Ag(100) surfaces is that we do not have to apply the external bias to transfer the charge across the interface. The dipole layer is formed in this case in the equilibrium state. This situation will allow for a simpler isolation of the intramolecular and interfacial effects. For example, some changes in Raman will be caused simply by the extra (or missing) charge on the molecule, which was reported in Ref.(Li et al., 2014). By virtue of this comparative analysis we will isolated the interfacial charge dynamics caused by vibrations, and rationalize the corresponding changes in Raman spectra.

3.2 PROJECT 2: GERS - Graphene Enhanced Raman Spectroscopy

SERS is predominantly associated with noble metals, which exhibit plasmonic behavior. From the point of view of understanding the chemical coupling in interfaces, plasmons complicate the analysis. From this perspective, graphene offers a perfect plasmon-free substrate, which is known to yield a much weaker, but purely chemical Raman enhancement (Zhang et al., 2016). The inclusion of graphene-based systems in this study will enable a direct comparison of the experimental and computational data, and the effects of CE to be directly quantified.

Along with graphene science, graphene-based Raman scattering (frequently called as GERS) is rapidly gaining importance in the research community, offering a great deal of tunability via external electric fields

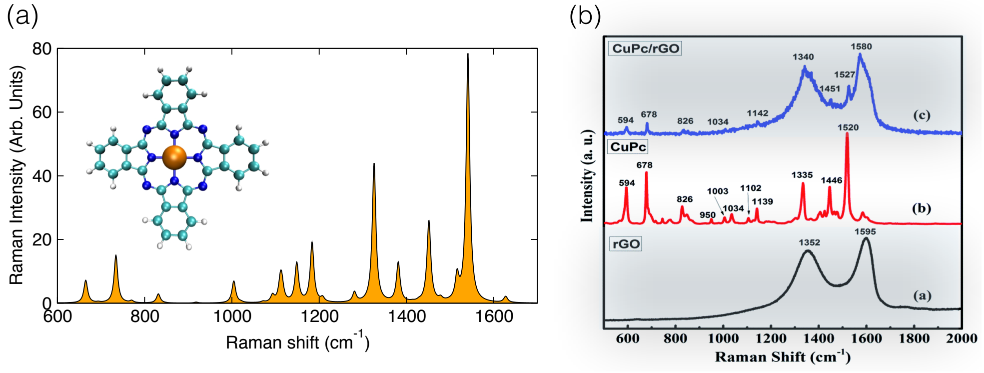

Figure 5: (a) The computed with SIESTA non-resonant Raman spectrum of CuPc (gas phase). (b) Experimental Raman of CuPc from Ref.(Kumar et al., 2017).

or *n/p* doping (Xu et al., 2011). There is so much promising research going on with numerous types of decorating used one graphene (Huang et al., 2015), that a chemically specific spectroscopic tool able to probe the interfacial coupling would be very attractive. GERS is very promising from this perspective due to our current understanding of the CE. It can reveal interfacial electronic structure and the interfacial charge transfer, serving as a tool for a chemically specific analysis of the tunability of graphene-based systems (Hao et al., 2013).

For this sub-project, we chose not a simple molecule, Copper Phthalocyanine (CuPc). CuPc has become one of the major molecules used for studying GERS (Zhang et al., 2016). It absorbs around 600-700 nm, which makes it resonant when using the standard 632 nm lasers. Our preliminary calculations with SIESTA for isolated CuPc show encouraging agreement with experimental data, shown in Fig.5.

3.2.1 Proposed work

1. ***Compute Raman spectra of CuPc on graphene under a range of external electric biases***

Similar to the case of C60@Au(111), we plan to investigate the impact of the surface on the Raman signature of the molecule and our ability to modulate the strength of the interfacial coupling by applying the bias.

Expected outcomes

The size of the molecule and its strong coupling to the surface of graphene should lead to well-pronounced changes in Raman spectra along with the associated dynamics of the charge density on the molecule and in the interface.

Expected problems

From the computational side, this molecule presents a challenge. It is rather big, and accommodating it on the surface of graphene requires a large area, leading to high computational costs. When we use Au or Ag as substrates, we can use the concept of frequency filtering. Basically, we ignore the dynamics of the metallic substrates, because their frequencies are so low that none of them overlaps with the vibrations of organic molecules. On the other hand, the G band of graphene is right where we expect the most interesting vibrational features of our molecules. Therefore, we have to compute vibrations and Raman responses of the entire system.

3.3 PROJECT 3: NCNQ vs. F4-TCNQ on graphene

While, CuPc is a very big system, other systems exist that can reveal charge transfer properties vis Raman scattering at significantly lower computational cost. We plan to study closely two molecules: TCNQ and F4-

TCNQ. These molecules placed on graphene (shown in Fig.6) are many times cheaper to compute, compared to CuPc. At the same time, F4-TCNQ has its own interesting features, because it is known to *p*-dope graphene (Misseeuw et al., 2016; Pinto et al., 2009). By comparing these two molecules we will be able to see the effect of the interfacial dipole layer on the Raman scattering in both non-resonant and resonant regimes.

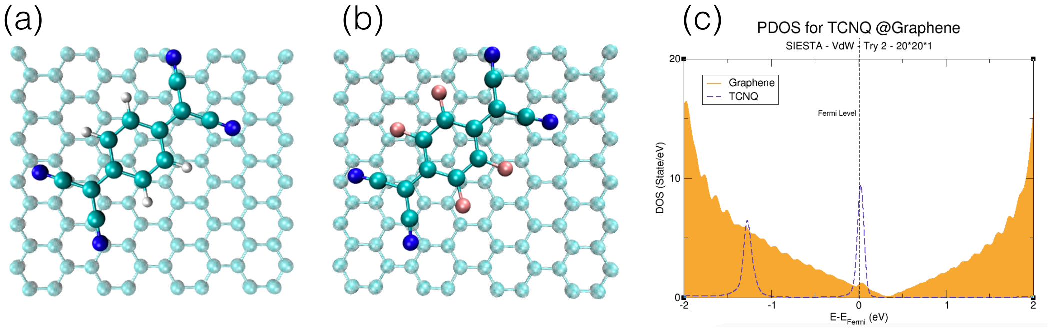

Figure 6: (a) Atomic structure of TCNQ on graphene. (b) Atomic structure of F4-TCNQ on graphene. (c) Electronic density of states of TCNQ on graphene. The LUMO state of TCNQ is right at the Fermi level of graphene, showing that TCNQ accepts charge, making graphene p-doped.

3.3.1 Proposed work

1. ***Compute Raman spectra of TCNQ and F4-TCNQ on graphene.***

- First, non-resonant Raman calculations will be carried out using the standard PBE functional in order to use this data as a reference. Then, we will include vdW interactions and draw conclusions about the impact of vdW interactions in the CE effect. - Raman calculations will be repeated for a number of different binding (physisorption) geometries. - Raman calculations will be performed in a wide range of applied external biases, which will allow us to control the amount of charge transfer. - In all types of calculations, we will look for the connections between the charge dynamics across the interface and the CE Raman signatures of it.

Expected outcomes This project will provide qualitative understanding of the interfacial coupling and the corresponding Raman response between the two molecules: TCNQ and F4-TCNQ. The later one, being fluorinated accepts more charge from the substrate, which gives us a straightforward way to relate the strength of CE with the charge transfer (interfacial dipole). This relatively small system will build up our expertise in Raman calculations of adsorbates on graphene in various contact geometries, helping us to reveal the impact of the contact on the strength of the non-covalent coupling and its signature in Raman.

4 JUSTIFICATION OF RESOURCES: 70,648 node hours (NH) on Stampede2

Our estimations are based on the usage of the software packages SIESTA and VASP, which has been optimized by the developers for MPI-like environments. We tested SIESTA and VASP on Stampede2 and were very satisfied with its parallel scaling, which is typical for DFT based computations (*please, see the scaling information in a separate document*). Due to the use of the "Divide and Conquer" approach, our calculations are trivially parallel: instead of running a single large calculation on many cores, we run big numbers of independent calculations, each using a single node. For example, for calculations of vibrations of a molecule with 24 atoms, we need to perform a structural relaxation first, and then do 24*3*2=144 calculations of forces in order to construct the dynamical matrix. Those 144 calculations are completely independent, and take just a few hours of wall time, thus can fill halls in the supercomputer schedule very efficiently. Moreover, for small systems we run concurrent jobs on a single node for more efficient utilizations of resources.

4.0.1 PROJECT 1

1.) **C60 Au(111)**

In this part of our project we will analyze the charge transfer at the Au - C60 interface and relate it to the previously computed Raman spectra. Overall, we have 11 (eleven) C60@Au systems to examine. Each system has 60 carbon atoms and 60 Au atoms. We include only the C60 vibrations in our analysis, which greatly reduces the costs. Each system has 180 vibrational modes that need to be analyzed. Both Raman- and IR-active vibrations will be taken into our analysis. A single calculation for our system costs about 2 NH. For 11 systems with 180 vibrational modes each, we will have 1980 cases to study. Each case will require calculations of charges (Bader analysis) with two amplitudes of the vibrational mode (”plus” and ”minus”), resulting in 3960 calculations.

Sub-total cost for this part is 8000 NH.

2.) **C60 Ag(100)**

For C60 at Ag(100) surface, we will perform Raman calculations, using the same approach as for the case of Au. The system consists of 160 atoms (60 C and 100 Ag). One single-point calculation takes about 3 node hours (NH). Only C atoms are included in the dynamical matrix. 60x6 = 360 are required to obtain vibrations. 180*2*3= 1080 calculations are required to compute non-resonant Raman spectra. Two systems will be considered: C60 bound via the 6-ring and 5-ring.

Sub-total cost for this part: $(200_{relaxation}\ NH + (360_{vibrations} + 1080_{Raman})*3\ NH = 4520\ NH)*2_{systems} = 9040\ NH$

TOTAL cost for PROJECT 1: 17,000 NH

4.0.2 PROJECT 2

Porphyrins are very and tough to compute large molecules. Calculations with graphene require a significant number of k-points for obtaining accurate electronic structure. Our molecule consists of 89 atoms, which lay on 240 C - atoms of graphene. A single calculation of this system takes about 4 NH. Unfortunately, the vibrational modes of both domains in this system overlap, which means that all atoms have to be taken into the dynamical matrix. Thus, the dynamical matrix will include 329 atoms, resulting in 987-6=981 vibrational modes.

Here are estimations for one Raman calculation:

- Structural relaxation - 200 NH
- Calculations of force constants - (4 NH) times (329 atoms) times (6 displacements) = 7,896 NH
- Calculation of Raman spectrum - (4 NH) times (987 vibrational modes) times (2 points for electric field perturbations) = 7,986 NH

Sub-total for one Raman calculations = 15,792 NH

We will restrict our analysis to only one molecular orientations (binding motif), and consider separately non-vdW and vdW interactions.

TOTAL cost for PROJECT 2: 15,792*2=31,584 NH

4.0.3 PROJECT 3

TCNQ and F4-TCNQ are much simpler molecules, which will enable us to study more adsorption geometries as well as examine the tunability of the charge transfer across the interface in the presence of external electric fields. This project will also allow for benchmarking of our SIESTA calculations with calculations done using VASP. An important aspect of this project is that we are comparing two molecules, one of which is a stronger electron acceptor than the other. The molecules of interest consist of 20 atoms, thus the dynamical matrix will yield to 20*3-6 = 54 vibrational modes.

Here are estimations for one SIESTA-based Raman calculation:

- Structural relaxation - 100 NH
- Calculations of force constants - (2 NH) times (20 atoms) times (6 displacements) = 240 NH
- Calculation of Raman spectrum - (2 NH) times (54 vibrational modes) times (2 points for electric field perturbations) = 216 NH
- One Raman calculation = 456 NH

Calculation will be done for 3 binding geometries, considering separately non-vdW and vdW interactions, for two molecules = 12 calculations. For both molecules Raman spectra will be calculated for a range of physisorption distances: by setting (enforcing) a fixed distance between the molecule and the graphene crossover from no-coupling to physisorption will be examined. Six calculations per molecule = 12 calculations. Electric field dependence will be studied with 10 values of external bias: -0.5, -0.4, -0.3, -0.2, -0.1, 0.1, 0.2, 0.3, 0.4, 0.5 V/Å. For the sake of saving computational resources, only one binding geometry will be considered and only non-vdW interactions, but still both molecules will be investigated = 20 calculations. Overall, we will perform 44 Raman calculations with SIESTA, which will require 20,064 NH.

VASP benchmarking.

We need VASP calculations only to make sure that our calculations of Raman are correct. Once we see that both SIESTA and VASP yield identical Raman spectra, we will continue calculations with SIESTA only. Thus VASP calculations will not be too costly. We only need Raman spectra of two molecules on graphene. The cost of VASP calculation is roughly double of SIESTA i.e. $\approx$ 1,000 NH per spectrum. For two spectra we will need 2,000 NH.

TOTAL cost for PROJECT 3: 22,064 NH

4.0.4 TOTAL ESTIMATES

Thus, the TOTAL computational needs for our project: **TOTAL = 17,000 + 31,584 + 22,064 = 70,648 node hours**

References

Adrian, FJ. "Charge transfer effect in surface-enhanced Raman scattering," *J. Chem. Phys.*, v. 77, 1982, p. 5302

Baibarac, M; Mihut, L; Preda, N; Baltog, I; Mevellec, J; Lefrant, S. "Surface-enhanced Raman scattering studies on C60 fullerene self-assemblies," *Carbon*, v. 43(1), 2005, p. 1–9

Campion, A; Kambhampati, P. "Surface-Enhanced Raman Scattering," *Chem. Soc. Rev.*, v. 27, 1998, p. 241–250

Cardona, M; Güntherodt, G. *Light scattering in solids II: Basic concepts and instrumentation*, Springer-Verlag, Berlin Heidelberg New York, chap. Resonance Phenomena, 1982

El-Khoury, PZ; Hess, WP. "Raman scattering from 1,3-propanedithiol at a hot spot: Theory meets experiment," *Chemical Physics Letters*, v. 581, 2013, p. 57–63

Ferraro, JR; Nakamoto, K; Brown, CW. *Introductory Raman spectroscopy*, Academic Press, Amsterdam ; Boston, 2nd ed., ISBN 978-0-12-254105-6, 2003

Fischer, SA; Apr, E; Govind, N; Hess, WP; El-Khoury, PZ. "Nonequilibrium Chemical Effects in Single-Molecule SERS Revealed by Ab Initio Molecular Dynamics Simulations," *The Journal of Physical Chemistry A*, v. 121(6), 2017, p. 1344–1350

Fleischman, M; Hendra, PJ; McQuillan, A. "Raman spectra of pyridine at a silver electrode," *Chem. Phys. Lett.*, v. 26, 1974, p. 163

Hao, Q; Morton, SM; Wang, B; Zhao, Y; Jensen, L; Jun Huang, T. "Tuning surface-enhanced Raman scattering from graphene substrates using the electric field effect and chemical doping," *Applied Physics Letters*, v. 102(1), 2013, p. 011102

Huang, S; Ling, X; Liang, L; Song, Y; Fang, W; Zhang, J; Kong, J; Meunier, V; Dresselhaus, MS. "Molecular Selectivity of Graphene-Enhanced Raman Scattering," *Nano Letters*, v. 15(5), 2015, p. 2892–2901

Jeanmaire, DL; Duyne, RPV. "Surface Raman spectroelectrochemistry: Part 1: Heterocyclic, aromatic, and aliphatic amines adsorbed on the anodized silver electrode," *J. Electroanal. Chem.*, v. 84, 1977, p. 1–20

Jensen, L; Aikens, CM; Schatz, GC. "Electronic structure methods for studying surface-enhanced Raman scattering," *Chem. Soc. Rev.*, v. 37, 2008, p. 1061–1073

Jensen, L; Zhao, LL; Autschbach, J; Schatz, GC. "Theory and method for calculating resonance raman scattering from resonance polarizability derivatives," *J. Chem. Phys.*, v. 123, 2005, p. 174110

Jensen, L; Zhao, LL; Schatz, GC. "Size-dependence of the enhanced raman scattering of pyridine adsorbed on ag_n (n=2-8,20) clusters," *J. Phys. Chem. C*, v. 111, 2007, p. 4756

Kim, K; Shin, KS. "Surface-enhanced Raman scattering: a powerful tool for chemical identification," *Analytical Sciences*, v. 27(8), 2011, p. 775

Kohn, W. "Nobel lecture: Electronic structure of matter - wave functions and density functionals," *Rev. Mod. Phys.*, v. 71, 1999, p. 1253

Kuhlman, AK; Zayak, AT. "Revealing interaction of organic adsorbates with semiconductor surfaces using chemically enhanced raman," *J. Phys. Chem. Lett.*, v. 5(6), 2014, p. 964–968

Kumar, S; Kaur, N; Sharma, AK; Mahajan, A; Bedi, RK. “Improved Cl_2 sensing characteristics of reduced graphene oxide when decorated with copper phthalocyanine nanoflowers,” *RSC Adv.*, v. 7(41), 2017, p. 25229–25236

Li, Y; Doak, P; Kronik, L; Neaton, JB; Natelson, D. “Voltage tuning of vibrational mode energies in single-molecule junctions,” *Proceedings of the National Academy of Sciences*, v. 111(4), 2014, p. 1282–1287

Lombardi, JR; Birke, RL. “Time-dependent picture of the charge-transfer contributions to surface enhanced Raman spectroscopy,” *The Journal of Chemical Physics*, v. 126(24), 2007, p. 244709

Misseeuw, L; Krajewska, A; Pasternak, I; Ciuk, T; Strupinski, W; Reekmans, G; Adriaensens, P; Geldof, D; Blockhuys, F; Van Vlierberghe, S; Thienpont, H; Dubruel, P; Vermeulen, N. “Optical-quality controllable wet-chemical doping of graphene through a uniform, transparent and low-roughness f4-tcnq/mek layer,” *RSC Adv.*, v. 6, 2016, p. 104491–104501

Moore, JE; Morton, SM; Jensen, L. “Importance of correctly describing charge-transfer excitations for understanding the chemical effect in SERS,” *J. Phys. Chem. Lett.*, v. 3(17), 2012, p. 2470–2475

Moskovits, M. “Surface-enhanced spectroscopy,” *Rev. Mod. Phys.*, v. 57, 1985, p. 783

Moskovits, M. “Persistent misconceptions regarding SERS,” *Phys. Chem. Chem. Phys.*, v. 15(15), 2013, p. 5301

Neugebauer, J; Reiher, M; Kind, C; Hess, BA. “Quantum chemical calculation of vibrational spectra of large molecules?Raman and IR spectra for Buckminsterfullerene,” *Journal of Computational Chemistry*, v. 23(9), 2002, p. 895–910

Pinto, H; Jones, R; Goss, JP; Briddon, PR. “p-type doping of graphene with F4-TCNQ,” *Journal of Physics: Condensed Matter*, v. 21(40), 2009, p. 402001

Postnikov, AV; Pages, O; Hugel, J. “Lattice dynamics of the mixed semiconductors (be,zn)se from first-principles calculations,” *Phys. Rev. B*, v. 71, 2005, p. 115206

Saikin, SK; Chu, Y; Rappoport, D; Crozier, KB; Aspuru-Guzik, A. “Separation of electromagnetic and chemical contributions to surface-enhanced raman spectra on nanoengineered plasmonic substrates,” *J. Phys. Chem. Lett.*, v. 1, 2010, p. 2740–2746

Schuck, PJ; Weber-Bargioni, A; Ashby, PD; Ogletree, DF; Schwartzberg, A; Cabrini, S. “Life Beyond Diffraction: Opening New Routes to Materials Characterization with Next-Generation Optical Near-Field Approaches,” *Advanced Functional Materials*, v. 23(20), 2013, p. 2539–2553

Soler, JM; Artacho, E; Gale, JD; Garcia, A; Junquera, J; Ordejon, P; Sanchez-Portal, D. “The SIESTA method for ab initio order-n materials simulation,” *J. Phys.: Condens. Matter*, v. 14(11), 2002, p. 2745

Stewart, S; Priore, RJ; Nelson, MP; Treado, PJ. “Raman Imaging,” *Annual Review of Analytical Chemistry*, v. 5(1), 2012, p. 337–360

Stiles, PL; Dieringer, JA; Shah, NC; Van Duyne, RP. “Surface-enhanced raman spectroscopy,” *Annual Review of Analytical Chemistry*, v. 1(1), 2008, p. 601–626

Umari, P; Pasquarello, A. “Infrared and Raman spectra of disordered materials from first principles,” *Diamond and Related Materials*, v. 14(8), 2005, p. 1255–1261

Valley, N; Greeneltch, N; Van Duyne, RP; Schatz, GC. "A Look at the Origin and Magnitude of the Chemical Contribution to the Enhancement Mechanism of Surface-Enhanced Raman Spectroscopy (SERS): Theory and Experiment," *The Journal of Physical Chemistry Letters*, 2013, p. 2599–2604

Xu, H; Chen, Y; Xu, W; Zhang, H; Kong, J; Dresselhaus, MS; Zhang, J. "Modulating the Charge-Transfer Enhancement in GERS using an Electrical Field under Vacuum and an n/p-Doping Atmosphere," *Small*, v. 7(20), 2011, p. 2945–2952

Zayak, AT; Choo, H; Hu, YS; Gargas, DJ; Cabrini, S; Bokor, J; Schuck, PJ; Neaton, JB. "Harnessing chemical raman enhancement for understanding organic adsorbate binding on metal surfaces," *J. Phys. Chem. Lett.*, v. 3(10), 2012, p. 1357–1362

Zayak, AT; Hu, YS; Choo, H; Bokor, J; Cabrini, S; Schuck, PJ; Neaton, JB. "Chemical raman enhancement of organic adsorbates on metal surfaces," *Phys. Rev. Lett.*, v. 106, 2011, p. 083003

Zhang, N; Tong, L; Zhang, J. "Graphene-Based Enhanced Raman Scattering toward Analytical Applications," *Chemistry of Materials*, v. 28(18), 2016, p. 6426–6435